⌘ *Author's Choice*

THE JOURNAL OF BIOLOGICAL CHEMISTRY VOL. 283, NO. 36, pp. 24826–24836, September 5, 2008

Demonstration of Short-lived Complexes of Cytochrome *c* with Cytochrome bc_1 by EPR Spectroscopy

IMPLICATIONS FOR THE MECHANISM OF INTERPROTEIN ELECTRON TRANSFER[*] [S]

Received for publication, March 19, 2008, and in revised form, July 8, 2008 Published, JBC Papers in Press, July 10, 2008, DOI 10.1074/jbc.M802174200

Marcin Sarewicz[‡], Arkadiusz Borek[‡], Fevzi Daldal[§], Wojciech Froncisz[‡], and Artur Osyczka[‡1]

From the [‡]Department of Biophysics, Faculty of Biochemistry, Biophysics, and Biotechnology, Jagiellonian University, 30-387 Kraków, Poland and the [§]Department of Biology, Plant Science Institute, University of Pennsylvania, Philadelphia, Pennsylvania 19104

One of the steps of a common pathway for biological energy conversion involves electron transfer between cytochrome *c* and cytochrome bc_1. To clarify the mechanism of this reaction, we examined the structural association of those two proteins using the electron transfer-independent electron paramagnetic resonance (EPR) techniques. Drawing on the differences in the continuous wave EPR spectra and saturation recoveries of spin-labeled bacterial and mitochondrial cytochromes *c* recorded in the absence and presence of bacterial cytochrome bc_1, we have exposed a time scale of dynamic equilibrium between the bound and the free state of cytochrome *c* at various ionic strengths. Our data show a successive decrease of the bound cytochrome *c* fraction as the ionic strength increases, with a limit of ~120 mM NaCl above which essentially no bound cytochrome *c* can be detected by EPR. This limit does not apply to all of the interactions of cytochrome *c* with cytochrome bc_1 because the cytochrome bc_1 enzymatic activity remained high over a much wider range of ionic strengths. We concluded that EPR monitors just the tightly bound state of the association and that an averaged lifetime of this state decreases from over 100 μs at low ionic strength to less than 400 ns at an ionic strength above 120 mM. This suggests that at physiological ionic strength, the tightly bound complex on average lasts less than the time needed for a single electron exchange between hemes *c* and c_1, indicating that productive electron transfer requires several collisions of the two molecules. This is consistent with an early idea of diffusion-coupled reactions that link the soluble electron carriers with the membranous complexes, which, we believe, provides a robust means of regulating electron flow through these complexes.

In biological energy conversion, the integrity of electron flow through the chains of redox cofactors is secured by the interactions between large membrane-embedded enzymatic complexes and small diffusible electron carriers (1). These diffusible carriers shuttle the electrons between the complexes. In mitochondria, cytochrome *c* connects cytochrome bc_1 (complex III) with cytochrome aa_3 oxidase (complex IV) (2, 3); in chloroplasts, plastocyanin connects cytochrome b_6f with photosystem I (4, 5); and in purple bacteria, cytochrome c_2 connects cytochrome bc_1 with the photosynthetic reaction center (6). Often, one chain contains multiple electron carriers with overlapping functions and properties. For example, cytochrome c_6 can replace plastocyanin (7), high potential iron-sulfur protein can replace various types of bacterial cytochromes *c* (6, 8), and membrane-attached cytochrome c_y can fulfill the function of soluble cytochrome c_2 (9). Clearly, nature has adopted several solutions to efficiently integrate the enzymatic complexes into physiologically functional units.

Despite this large diversity of electron carriers, a common pattern can be found in the architecture of the protein-protein interaction. Typically, the small electron carriers contain just one redox center asymmetrically embedded within the protein so that it faces closely one side of the molecule. This side acts as the docking site and comes into close contacts with the docking site of the membranous complex (*i.e.* that portion of its surface where the other redox center is partially exposed) (10, 11), as shown in Fig. 1 for the interaction between soluble cytochrome *c* and membranous cytochrome bc_1. In this way, a distance of less than 14 Å, and thereby an electron transfer at physiologically competent rates, can be achieved between the two interacting redox centers (12, 13). A diffusible electron carrier alternates between the complexes using the same side in every interaction.

This raises an engineering question as to how the right orientation of the two interacting redox proteins is achieved. Multistep mechanisms are usually envisaged (10, 14–16). The first step is a random collision that depends solely on the translational diffusion of proteins. The randomly formed complex may develop to the encounter complex, or it may dissociate (16). The encounter complex may further evolve into the final, tightly bound complex. All of these processes may be facilitated by the long-range electrostatic attractive forces between oppositely charged residues of the docking surfaces (14, 16–18). This is quite well established for many interactions involving cytochromes *c* (2, 10, 19) but is much less certain for some other interactions (for example, those with high potential iron-sulfur protein (20, 21)). Short-range hydrophobic interactions and hydrogen bonding may also contribute to binding, especially in

* This work was supported, in whole or in part, by National Institutes of Health Grant GM 38237 (to F. D.). It was also supported by a Wellcome Trust International Senior Research Fellowship (to A. O.) and U. S. Department of Energy Grant ER20052 (to F. D.). The costs of publication of this article were defrayed in part by the payment of page charges. This article must therefore be hereby marked "*advertisement*" in accordance with 18 U.S.C. Section 1734 solely to indicate this fact.

⌘ *Author's Choice*—Final version full access.

[S] The on-line version of this article (available at http://www.jbc.org) contains supplemental material, Fig. S1, Table S1, and additional references.

[1] To whom correspondence should be addressed. Tel.: 48-12-664-6348; E-mail: osyczkaa@biotka.mol.uj.edu.pl.

the final steps of association when the distance between the proteins is the shortest (11).

We thus can appreciate many of the structural and kinetic details about the interactions between specific redox proteins (see examples in Refs. 2, 10, 11, and 19–27). Yet, the meaning of the dynamic equilibrium between the various steps of molecular association in the context of the mechanism of electron transfer is not as well understood.

Addressing this question in our experimental approach, we have used electron paramagnetic resonance techniques (28–30) to examine the dynamics of structural association of cytochrome *c* with cytochrome bc_1. We have specifically modified bacterial and mitochondrial cytochromes *c* with spin label at differently located positions with respect to the docking site. We then used continuous wave (CW)[2] EPR and saturation recovery (SR) ERP measurements to verify an orientation of cytochrome *c* in its interaction with cytochrome bc_1. Finally, we used CW and SR EPR to expose a time scale of dynamic equilibrium between the bound and free states of cytochrome *c* at various ionic strengths. The proposed estimates on the averaged lifetime of the cytochrome *c*-cytochrome bc_1 complex shed light on the mechanisms of electron transfer between these two proteins. They imply that the reactions are diffusion-coupled under physiological conditions. Possibly, this mechanism is more general and applies to other protein-protein interactions in the redox systems.

EXPERIMENTAL PROCEDURES

Bacterial Strains and Plasmids—*Rhodobacter* (*Rba.*) *capsulatus* strain pMTS1/MT-RBC1 overproduces wild type cytochrome bc_1 (31), pC-M183K/MT-RBC1 overproduces cytochrome bc_1 with mutation M183K in cytochrome c_1 (32), and FJ2 lacks cytochromes c_2 and c_y (33). Plasmid pHM2 is a derivative of pBSII containing a copy of *cyc*A (34), and pHM14 is a derivative of pRK415 containing a wild type copy of *cyc*A (35).

Preparation of Single Cysteine Mutants of Cytochrome c_2—*Rba. capsulatus* strains with mutated cytochrome c_2 were generated as described previously (33–36). The mutations were constructed by site-directed mutagenesis using the QuikChange system from Stratagene and the plasmid pHM2 as the template DNA. The following mutagenic primers were used to introduce single cysteine mutations (F and R denote forward and reverse primers, respectively): 5′-GGC TTC GCC TGG TGC GAG GAA GAC ATC G-3′ (T68C-F), 5′-GTC TTC CTC GCA CCA GGC GAA GCC CGA G-3′ (T68C-R); 5′-GGC GTT CAA ACT CTG CAA GGG CGG CGA AGA CG-3′ (A101C-F), 5′-CTT CGC CGC CCT TGC AGA GTT TGA ACG CCA TG-3′ (A101C-R). After sequencing, the appropriate DNA fragments bearing the desired mutation and no other mutations were exchanged with their wild type counterparts in the expression vector pHM14 using the restriction enzymes KpnI and HindIII. The mutated variants of pHM14 were then introduced into FJ2 strain (*cyc*A and *cyc*Y deletion background) via triparental crosses. The presence of engineered mutations was confirmed by sequencing the plasmid DNA isolated from the mutated *Rba. capsulatus* strains.

Isolation of Cytochrome c_2 and Cytochrome bc_1—Cytochrome c_2 was isolated from *Rba. capsulatus* FJ2 strain complemented with wild type or mutated pHM14 as described (37), except that the chloroform extraction step was omitted. Cytochrome bc_1 complex was isolated from *Rba. capsulatus* MT-RBC1 strain complemented with wild type or mutated pMTS1 as described (38). The purity of isolated proteins was checked with SDS-PAGE. A concentration of cytochrome *c* was determined spectrophotometrically using ascorbate-reduced *minus* ferricyanide-oxidized spectrum and an extinction coefficient ϵ_{550} of 18.5 $mM^{-1}cm^{-1}$ (39). A concentration of cytochrome bc_1 was determined from the ascorbate-reduced *minus* ferricyanide-oxidized spectra (for the wild type) or from the dithionite-reduced *minus* ferricyanide-oxidized spectra (for the M183K mutant) using an extinction coefficient $\epsilon_{551\text{-}542\ nm}$ of 20 $mM^{-1}cm^{-1}$ (38).

Spin Labeling of Cytochromes c—Prior to spin labeling, cytochromes c_2 A101C and T68C were bound to thiopropyl-Sepharose (GE Healthcare) and eluted with 50 mM dithiothreitol. This was followed by gel filtration on Sephadex G-25 (equilibrated with 50 mM Tris-HCl, pH 8.0, 100 mM NaCl) to remove dithiothreitol. Immediately after elution of cytochrome c_2, methanethiosulfonate spin label, selective toward thiol groups (40), was added from acetonitrile stock to obtain a 10-fold molar excess over cytochrome c_2. The sample was incubated at room temperature for 1 h and then dialyzed against 5 mM Tris buffer, pH 7.4, to remove an excess of unreacted spin label. Yeast iso-1 cytochrome *c* (Sigma) was labeled at its native Cys-102 with methanethiosulfonate spin label using the same reaction conditions and dialysis as in the case of cytochrome c_2. A monoderivative of horse heart cytochrome *c* (Sigma) labeled at Lys-86 with succinimidyl-2,2, 5,5-tetramethyl-3-pyrroline-1-oxyl-carboxylate was obtained as described elsewhere (41). The molar ratio of the attached spin label (SL) to protein was determined by comparison of the double integrated EPR spectra of spin-labeled cytochrome *c* with the EPR spectrum of the TEMPOL standard. The concentration of TEMPOL was determined spectrophotometrically using an extinction coefficient, ϵ_{428}, of 13.4 $M^{-1}cm^{-1}$ (42). The concentration of cytochrome c_2 was determined spectrophotometrically as described above, and the same procedure was used for two mitochondrial cytochromes. The samples with a molar ratio of 1:1 of SL per cytochrome *c* molecule were used in further experiments (substoichiometrically labeled samples were discarded).

Continuous Wave Measurements (CW EPR) and Analysis—Spin-labeled cytochromes *c* were mixed with *Rba. capsulatus* cytochrome bc_1 in 5 mM Tris, pH 7.4, and different ionic strengths were adjusted by adding varying amount of concentrated NaCl. Final concentrations of cytochrome *c* and cytochrome bc_1 were 20 and 40 μM, respectively. This ratio was chosen to satisfy the reported 1:2 stoichiometry of the binding of cytochrome *c* to cytochrome bc_1 (11). At this ratio, the absolute concentration of labeled cytochrome c_2 yields a satisfactory level of signal-to-noise with the low amount of unbound cytochrome c_2 that contributes to the EPR spectra.

[2] The abbreviations used are: CW, continuous wave; SR, saturation recovery; SL, spin label; A101C-SL, cytochrome c_2 labeled with SL at position 101; T68C-SL, cytochrome c_2 labeled with SL at position 68; *Rba.*, *Rhodobacter*; TEMPOL, 4-hydroxy-2,2,6,6-tetramethylpiperidine-1-oxyl.

CW EPR spectra were recorded at room temperature on a Bruker Elexsys E580 spectrometer equipped with a super high-Q resonator. Samples were measured in flat quartz cells (0.4 × 4 mm, inner diameter; VitroCom Inc.) with total active volume of 30 μl. The parameters were: microwave frequency 9.87 GHz, microwave power 19.95 milliwatts, modulation amplitude/frequency 1 G/100 kHz, sweep width 150 G, time constant 20.48 ms, sweep time 20.97 s/scan, resolution 4096 points/scan (number of scans was at least 25). The fraction of cytochrome *c* bound to cytochrome bc_1 at a given ionic strength was calculated using the multiple linear regression method as described previously (43). Briefly, the measured spectrum was linearly decomposed into two parts corresponding to the spectra of free and bound cytochrome *c* defined as reference. The reference spectrum of free cytochrome *c* was a spectrum of spin-labeled cytochrome *c* measured in the absence of cytochrome bc_1 in 5 mM Tris, pH 7.4. The reference spectrum of bound cytochrome *c* was a spectrum of spin-labeled cytochrome *c* measured in the presence of a 2-fold molar excess of cytochrome bc_1 in 5 mM Tris, pH 7.4. The latter should be considered as the spectrum of predominantly rather than fully bound cytochrome *c*, because it contains a contribution from the residual unbound cytochrome *c*. This made the bound fraction of cytochrome *c* slightly overestimated. Nevertheless, the concentrations of calculated free and bound cytochrome *c* stayed within the same order of magnitude as the true value, as described in detail elsewhere (43).

Saturation Recovery Measurements (SR EPR) and Analysis—Samples of spin-labeled cytochrome *c* with cytochrome bc_1 were prepared in a manner similar to CW EPR measurements, except that higher concentrations of proteins were used (34 and 63 μM for cytochrome *c* and cytochrome bc_1, respectively). Protein solutions were placed in a thin, gas-permeable methylpentene capillary. An oxygen-free atmosphere was obtained by flushing pure nitrogen gas through the resonator for at least 20 min before measurement. The measurements were performed on a home-made pulse spectrometer (44) operating at X-band using 1-mm loop-gap resonator (45). The SR curves were recorded at the central EPR line ($m_I = 0$) using the following parameters: pumping power 0.35 milliwatt, observing power 0.03 milliwatt, pulse length 450 ns, spectrometer dead time 350 ns. SR curves were digitized with 1024 points at a rate of 50 MHz. The number of accumulations varied from 10,000 to 50,000 to obtain a satisfactory signal-to-noise ratio.

All samples were measured three times, and the acquired SR curves were fitted to the single and double exponential recovery model using a nonlinear Levenberg-Marquardt algorithm implemented in the Dataplot program (Statistical Engineering Division, National Institute of Standards and Technology) (46) or PSI-Plot, a scientific spreadsheet and technical plotting program that implements the Levenberg-Marquardt and simplex, Powell methods and can perform a global analysis for a set of recovery curves. When the exchange rate between the bound and free cytochrome *c* at low ionic strength condition is slower than the spin lattice relaxation rate of the most slowly relaxing component, the biexponential recovery of SR curve is observed. One component of the recovery should be characterized by the time constant equal to the spin lattice relaxation time measured for cytochrome c_2 A101C in buffer in the absence of cytochrome bc_1. The second time constant should be equal to the spin lattice relaxation time of fully bound cytochrome c_2 to cytochrome bc_1. In our case, both exchange rates (association and dissociation) are comparable with the longitudinal relaxation rates of SL attached to cytochrome c_2. Thus, the relaxation time constants τ_1 and τ_2 and the amplitudes *a* and *b* of both exponents are functions of the intrinsic relaxation and the exchange rates. Therefore, we performed a fit to the following equation,

$$f(t) = a \cdot \exp(-t/\tau_1) + b \cdot \exp(-t/\tau_2) + c \qquad \text{(Eq. 1)}$$

where $f(t)$ is signal amplitude at time *t* and *c* is the constant representing the base line of the SR curve.

The calculated values of *a* and *b* depend also on the initial value of the magnetization vector after the pump pulse. The exchange rates were estimated from time constants obtained using formulas from Hansen and Led (47). It should be noted that amplitudes *a* and *b* are not directly proportional to the concentration of free and bound cytochrome *c*. Other details on the SR EPR methodology are found in the supplemental material.

Cytochrome bc_1 Enzymatic Activity Measurements—Steady-state enzymatic activity was assayed by measuring the decylubiquinol-dependent reduction of cytochrome *c* as described previously (31). Buffer and sample conditions were: 20 μM cytochrome *c*, 20 μM decylubiquinol, 5 nM cytochrome bc_1, and 5 mM Tris-HCl, pH 7.8, containing 0.01% dodecyl maltoside. Different ionic strengths were adjusted by the addition of NaCl from a concentrated stock solution. Cytochrome c_2 (E_{m7} = 360 mV) is predominantly reduced under ambient atmosphere. Therefore, prior to the assays, cytochrome c_2 was oxidized with an excess of ferricyanide and then passed through Sephadex G-25 to remove the oxidant. Such sample was used in the activity assays. (We determined that cytochrome c_2 remains oxidized at about 70% shortly after the removal of ferricyanide, a state that is stable for several hours.) Mitochondrial cytochromes *c* were used in the activity assays without any additional treatment.

Model of the Cytochrome c_2-Cytochrome bc_1 Complex—The putative model of cytochrome c_2 bound to cytochrome bc_1 was constructed by superposition of *Rba. capsulatus* cytochrome bc_1 structure (Protein Data Bank ID code: 1ZRT) (48) with the corresponding chains from the structure of yeast cytochrome bc_1 with bound cytochrome *c* (Protein Data Bank ID code: 1KYO) (11). The structure of *Rba. capsulatus* cytochrome c_2 (Protein Data Bank ID code: 1C2R) (49) was aligned to the structure of cytochrome *c* chain from the 1KYO structure. The single cysteine substitutions of residues 68 and 101 and the stick model of the spin label was built into the structure of cytochrome c_2 using the PyMOL molecular graphics system (50).

RESULTS

Properties of Mutated Cytochromes c_2—The single cysteine substitutions T68C and A101C yield photosynthetically competent *Rba. capsulatus* strains (FJ2 strains complemented with mutated pHM14) producing cytochrome c_2, which has a wild

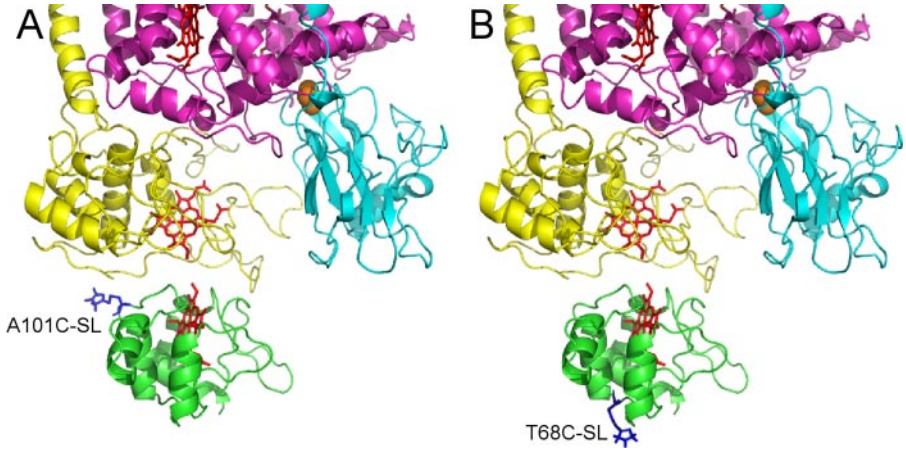

FIGURE 1. **Ribbon model of possible complex of cytochrome c_2 with cytochrome bc_1 in *Rba. capsulatus*.** Cytochrome c_2 (*green*) interacts directly with cytochrome c_1 (*yellow*) of the catalytic core of cytochrome bc_1, which also contains two other subunits: iron-sulfur protein (*turquoise*) and cytochrome *b* (*magenta*). *A* and *B* show attachment of SL (*blue*) in two cysteine mutants of cytochrome c_2, A101C and T68C, respectively. Hemes are shown in *red* and iron-sulfur clusters in *orange*.

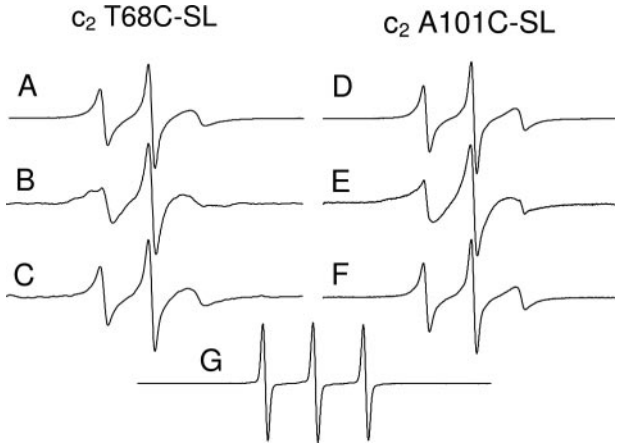

FIGURE 2. **CW EPR spectra of spin-labeled *Rba. capsulatus* cytochrome c_2.** Spectra of T68C-SL (*left column*) and A101C-SL (*right column*) were recorded in 5 mM Tris-HCl, pH 7.4, in the absence (*A* and *D*) or presence of cytochrome bc_1 (*B* and *E*) and in 5 mM Tris-HCl, 300 mM NaCl, pH 7.4, in the presence of cytochrome bc_1 (*C* and *F*). Concentrations of proteins were: 20 μM cytochrome c_2 (*A–F*) and 40 μM cytochrome bc_1 (*B*, *C*, *E*, and *F*). For comparison, the spectrum of free spin label is shown in *G*.

type spectra and electrochemical properties of high potential cytochrome *c* (data not shown). Cytochromes c_2 modified with spin label have properties similar to the wild type cytochrome c_2 when used as substrates for cytochrome bc_1 in the enzymatic activity assays (supplemental Table S1).

CW EPR of Spin-labeled Cytochromes c in the Absence and Presence of Cytochrome bc_1—In general terms, the overall shape of the EPR spectrum of SL reflects its mobility (28, 51). In practice this means that the observable changes in the EPR spectra can often be related to the changes in the mobility of SL, which may provide useful information about the structure and dynamics of a studied system. In Fig. 2 we used these considerations in comparing the CW EPR spectra of methanethiosulfonate spin-labeled A101C and T68C mutants of cytochrome c_2 (see Fig. 1 for positions of those mutations) recorded at room temperature in buffer without and with its redox partner, cytochrome bc_1.

In buffer alone, SL attached to either position (Fig. 2, *A* and *D*, for T68C and A101C, respectively) has a relatively high mobility, which is consistent with a surface location of those two positions (see Fig. 1). This mobility is, however, smaller than a mobility of the free SL in solution, where the typical spectrum has *three narrow lines* (Fig. 2*G*). The broadening of the lines in the EPR spectrum of T68C-SL and A101C-SL reflects restrictions in motion imposed by the attachment of SL to a much larger molecule of cytochrome c_2.

When spin-labeled cytochrome c_2 is mixed with isolated cytochrome bc_1 in a solution at low ionic strength, the EPR spectra become further broadened and additional components appear. For T68C-SL, at least three new components of slower mobility can clearly be recognized in the lowest field EPR line (Fig. 2*B*), whereas the significant broadening of A101C-SL comes from superposition of at least two components of different mobility (Fig. 2*E*). Overall, these changes reflect additional restrictions to the SL motion, which appear to come from the direct interaction of cytochrome c_2 with cytochrome bc_1 and a formation of the complex between these two proteins. This is further confirmed by the observation that changes in the SL line shapes induced by the presence of cytochrome bc_1 at the low ionic strength disappear at the high ionic strength. For both T68C-SL and A101C-SL, spectra recorded at high salt concentration in the presence of cytochrome bc_1 (Fig. 2, *C* and *F*, respectively) are similar to those registered in the absence of cytochrome bc_1 (Fig. 2, *A* and *D*). Such a behavior is consistent with the well known electrostatic nature of the cytochrome *c*-cytochrome bc_1 interaction and its diagnostically strong dependence on the ionic strength. We conclude that CW EPR conveniently detects the interaction of cytochrome c_2 with cytochrome bc_1 under conditions of low ionic strength.

The interaction of cytochrome bc_1 with other cytochromes *c* can be monitored in a similar manner. For example, clear changes in the shape of CW EPR spectra of SL are induced by the addition of cytochrome bc_1 to mitochondrial homologues of bacterial cytochrome c_2 (horse cytochrome *c* labeled at Lys-86 or yeast cytochrome *c* labeled at Cys-102) (supplemental Fig. S1). Again, these changes are heavily dependent on ionic strength and as such can be interpreted as reflecting a formation of a complex between the two proteins.

The predicted structure of the cytochrome c_2-cytochrome bc_1 complex shows Ala-101 close to and Thr-68 remote from the docking surface (Fig. 1). In principle, such a difference in the location of those positions within the complex might be reflected by distinct measurable effects in the CW EPR spectra of T68C-SL and A101C-SL complexed with cytochrome bc_1. Indeed, measurements taken at low ionic strength show that the shapes of CW EPR spectra of T68C-SL and A101C-SL differ

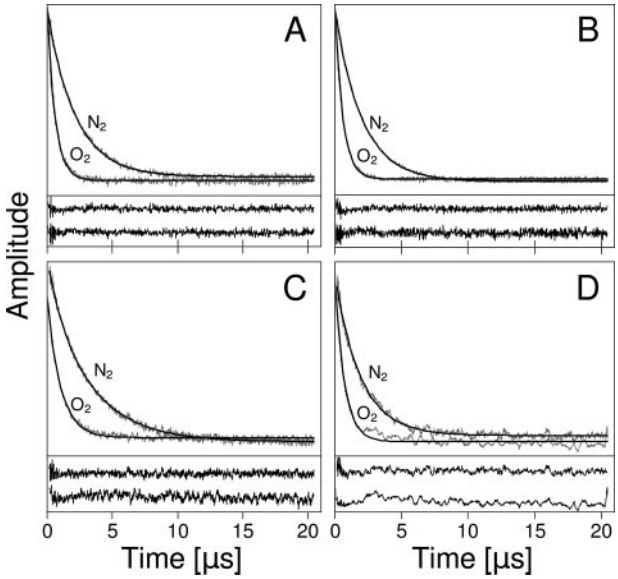

FIGURE 3. **SR EPR recovery curves of spin-labeled *Rba. capsulatus* cytochrome c_2.** Curves of A101C-SL (*left*) and T68C-SL (*right*) were recorded in the absence (*A* and *B*) or presence of cytochrome bc_1 (*C* and *D*). N_2 and O_2 denote traces registered in the absence and presence of molecular oxygen, respectively. Data in *A*, *B*, and *D* were best fitted with single exponential function (*solid lines*), whereas the data for N_2 (in *C*) were best fitted with double exponential function (*line*). Concentrations of proteins were: 34 μM cytochrome c_2 (*A–D*) and 63 μM cytochrome bc_1 (*C* and *D*). The corresponding residuals for all fits are shown *below* the graphs. In each panel, the *upper* and *lower traces* represent the residuals for curves measured in N_2 and O_2, respectively.

from each other more profoundly in the presence of cytochrome bc_1 (Fig. 2, *B versus E*) than in its absence (Fig. 2, *A versus D*). The difference seen in Fig. 2 in *spectrum B versus E* is assumed to reflect the geometric arrangement of cytochrome c_2 in complex with cytochrome bc_1. This was further supported by the results of SR measurements (see below).

SR EPR of Spin-labeled Cytochrome c_2 in the Absence and Presence of Cytochrome bc_1—Measurements of the accessibility of SL to paramagnetic quenchers provide information on the degree of exposure of SL to a quencher-penetrable phase, which can often reveal details about the geometric location of SL (52–54). In practice, the exposure of SL can be estimated from a comparison of the SR recovery rates measured in the presence and the absence of the paramagnetic molecule. Typically, the recovery rates depend on an intrinsic spin lattice relaxation and, if quencher is present and SL is accessible to the quencher, on Heisenberg exchange between the SL and the quencher (see supplemental Equation 3). Because the Heisenberg exchange significantly enhances the recovery rate, the effective rate of the quencher-exposed SL is going to be much faster in the presence of the quencher than in its absence. Indeed, both T68C-SL and A101C-SL, as having labeled solvent-exposed residues (Fig. 1), show clear enhancement of the SL recovery rates in the presence of paramagnetic oxygen (Fig. 3, *A* and *B*; Table 1).

In the absence of cytochrome bc_1, the extent of this enhancement and the absolute values of the relaxation rate remain essentially the same for both labeled positions (Fig. 3, *A* and *B*; Table 1). We note that the SR curves are best fitted with a single exponent. In contrast, clear differences in the relaxation behavior of T68C-SL and A101C-SL arise upon the addition of cytochrome bc_1 (Fig. 3, *C* and *D*; Table 1). The relaxation rates in T68C-SL change only very slightly, and a SR recovery remains single exponential. In A101C-SL, a SR curves becomes clearly biexponential with two different time constants. Although those time constants can be interpreted as reflecting the presence of cytochrome c_2 under dynamic exchange between bound and free states, they do not represent intrinsic relaxation times of the corresponding states of cytochrome *c*, because they are shortened by the exchange itself (see supplemental material).

TABLE 1
Spin lattice relaxation times (T_1) of the spin label attached to cytochrome c_2 (T68C or A101C) in the presence and absence of cytochrome bc_1 in low ionic strength buffer

Mutant	Buffer (T_1)		Cytochrome bc_1 (T_1)	
	N_2[a]	O_2[b]	N_2[c]	O_2[d]
	μs	μs	μs	μs
A101C	2.14 ± 0.04	0.61 ± 0.01	3.27 ± 0.18 1.70 ± 0.25	0.96 ± 0.12
T68C	2.00 ± 0.03	0.59 ± 0.01	1.9 ± 0.4	0.59 ± 0.07

[a] In the absence of cytochrome bc_1 under nitrogen.
[b] In the absence of cytochrome bc_1 in the equilibrium with air.
[c] In the presence of cytochrome bc_1 under nitrogen.
[d] In the presence of cytochrome bc_1 in the equilibrium with air.

The biexponential relaxation of A101C-SL, but not T68C-SL, reveals that SL attached to A101C, unlike the SL attached to T68C, experiences significant mobility restriction when cytochrome c_2 is in complex with cytochrome bc_1. Conceivably, these restrictions are caused by a proximity of Ala-101 to the surface of cytochrome c_1 in the complex (Fig. 1*A*). This could slow down a local rotation of SL in A101C-SL and thereby decrease its intrinsic relaxation rate (55). Thr-68 protrudes much further away from the surface of cytochrome c_1 (Fig. 1*B*), and thus SL in T68C-SL remains sensitive only to damped rotational tumbling of the whole protein complex (changes seen in the CW EPR spectrum), but its local surface motion is not changed (no effect on the relaxation time). Clearly, the SR data add to the CW data in showing ternary effects resulting from the association of cytochrome c_2 with cytochrome bc_1.

The ternary effects are also evident in the measurements of the Heisenberg exchange rate with oxygen (W_{ex}) and its dependence on ionic strength (Fig. 4). The W_{ex} values for A101C-SL rise with increasing salt concentrations and reach the maximum level at ~60 mM NaCl. In contrast, the W_{ex} values for T68C-SL remain similar at both low and high ionic strength at the level converging with the maximum level of A101C-SL. These results, interpreted in light of the strong ionic strength dependence of the cytochrome *c*-cytochrome bc_1 interaction, indicate that changes in the accessibility of oxygen to SL (changes in the W_{ex} values) in A101C occur concomitantly with the formation of the cytochrome *c*-cytochrome bc_1 complex in which the proximal to Ala-101 surface of cytochrome c_1 (see Fig. 1*A*) effectively shields the access to molecular oxygen. At the same time, the accessibility of T68C-SL to oxygen is not affected by binding to cytochrome bc_1, which is what can be expected if cytochrome c_2 binds in an orientation directing Thr-68 away from the surface of cytochrome c_1 (see Fig. 1*B*), thus excluding any shielding effects.

Overall, the results presented thus far consistently indicate that the applied EPR measurements distinguish differences in local

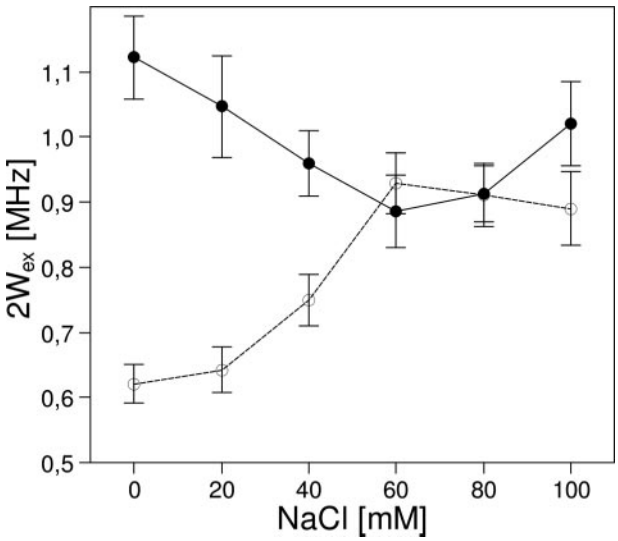

FIGURE 4. **The accessibility of molecular oxygen to spin-labeled cytochrome c_2 in the presence of cytochrome bc_1.** The extent of Heisenberg exchange rate (W_{ex}) between molecular oxygen and A101C-SL (*open circles*) or T68C-SL (*closed circles*) is plotted as a function of NaCl concentration. W_{ex} was obtained from the SR EPR recovery curves similar to those shown in Fig. 3, as described under "Experimental Procedures."

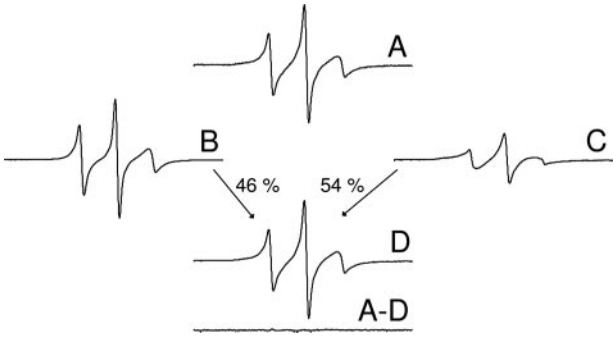

FIGURE 5. **Estimation of the fraction of spin-labeled cytochrome c_2 bound to cytochrome bc_1.** The spectrum of A101C-SL measured in the presence of a 2-fold molar excess of cytochrome bc_1 at 40 mM of NaCl (*A*) was linearly decomposed into parts representing free (*B*) and predominantly bound (*C*) cytochrome c_2 to obtain the proportions shown in the figure. The sum of spectra *B* and *C* in those proportions yields spectrum *D*, which is of identical shape to experimental spectrum *A*. The difference between spectrum *A* and *D* gives a residual without a trace of EPR spectrum-like structure.

environments of Ala-101 and Thr-68 of cytochrome c_2 interacting with cytochrome bc_1. Cytochrome c_2 appears to face its redox partner from the exposed heme edge side (Ala-101 side), which generally agrees with the predicted orientation of cytochrome c_2 in the complex with cytochrome bc_1 (Fig. 1). Given these experimental confirmations, the dynamics of structural association of cytochrome *c* with cytochrome bc_1 can be examined.

Ionic Strength Dependence of Binding of Cytochrome c to Cytochrome bc_1 as Seen by CW and SR EPR—The observed changes in the shape of the EPR spectrum (Fig. 2) and the relaxation rates (Fig. 3) of spin-labeled cytochrome *c* upon its binding to cytochrome bc_1 can be used conveniently to expose a dynamic equilibrium between the bound and the free state of cytochrome *c*. Our approach was based on two methods that monitor the interaction of cytochrome *c* with cytochrome bc_1 at two different time domains. The first method was a linear decomposition of the CW EPR spectra, as shown in Fig. 5 (43); the second method was a nonlinear fitting of a biexponential function to the SR curves (see "Experimental Procedures" for details). Because the binding between the two redox partners is in part controlled by electrostatic interactions, (23–27, 56, 57) the changes in the ionic strength were used to effectively manipulate the binding equilibrium of the reaction.

Fig. 6 shows the fraction of bound cytochrome *c* normalized to the predominantly bound fraction at 5 mM Tris buffer as a function of ionic strength obtained with the CW EPR method. As expected from the electrostatic character of the binding, three tested soluble cytochromes (cytochrome c_2, horse cytochrome *c*, and yeast cytochrome *c*) showed a successive decrease of the bound fraction as the ionic strength increased. We note that the profile for cytochrome c_2 does not depend on the SL attachment site (Fig. 6*A*).

The sigmoidal dependence reveals a limit of around 120 mM NaCl above which the minimal amount, or essentially no bound cytochrome *c*, can be detected in the CW EPR spectrum (this limit is 120 mM NaCl for cytochrome c_2, 90 mM for horse cytochrome *c*, 150 mM for yeast cytochrome *c*). The profile with no bound fraction at high salt concentrations is seen for cytochrome c_2 and horse cytochrome *c*, but for yeast cytochrome *c*, a 30% bound fraction remains even at a very high salt concentration (Fig. 6*B*).

The differences between yeast cytochrome *c* and the two other soluble cytochromes may arise from the difference in the relative contribution of electrostatic and hydrophobic components to the binding. If the nonpolar interactions are generally stronger in the yeast system, as already indicated (23, 57), they may not be easily eliminated by ionic strength and thus may leave a significant fraction of bound cytochrome *c* at high ionic strength. Indeed, the contributions of the electrostatic and hydrophobic components may vary in different systems, which seems to be at the root of the diversity of the observed modes of protein-protein interactions (20, 21, 58, 59).

To test the effect of the redox state of cytochrome c_1 on the binding of cytochrome c_2, a mutant M183K was used. In this form, cytochrome c_1 has a redox potential lowered some 400 mV *versus* wild type (32) and under the applied experimental conditions remains oxidized before and after mixing with reduced cytochrome c_2. The comparison shown in Fig. 6*C* demonstrates that although the redox state of cytochrome c_1 has some effect on the binding equilibrium, the range of ionic strength with no bound cytochrome *c* detected by CW EPR is essentially the same for oxidized and reduced cytochrome c_1.

The analysis of the relaxation behavior of A101C-SL in the presence of cytochrome bc_1, summarized in Table 2, shows that the biexponential recovery can be seen only up to ~40 mM NaCl. Further, both relaxation time constants successively decrease as the ionic strength increases from 0 to 40 mM NaCl. This collapse of the two relaxation times into one can be attributed to a successive decrease of the bound cytochrome *c* as monitored by SR EPR.

The two components that contribute to the SR curve are resolvable only if they undergo exchange at rates slower than the longitudinal SL relaxation rate (around $10^5\ s^{-1}$ or more). However, if the exchange rate approaches or becomes faster

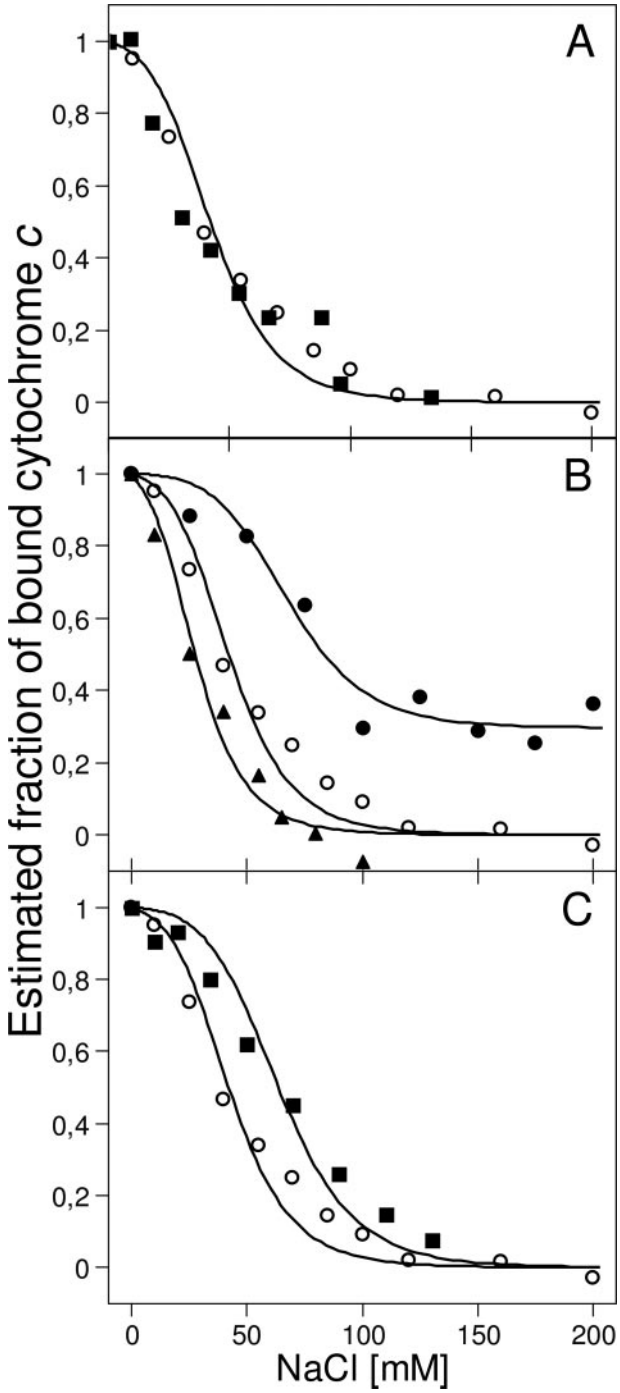

FIGURE 6. **Effect of ionic strength on binding of cytochrome *c* to cytochrome bc_1 as monitored by CW EPR.** *A*, normalized fraction of A101C-SL (*open circles*) and T68C-SL (*closed squares*) bound to wild type cytochrome bc_1. *B*, K86-SL (horse cytochrome *c* labeled with SL at position 86; *closed triangles*) and C102-SL (yeast cytochrome *c* labeled with SL at position 102; *closed circles*) bound to wild type cytochrome bc_1. Data for A101C-SL (*open circles*) are replotted from *A* for comparison. *C*, normalized fraction of A101C-SL bound to the mutant c_1-M183K of cytochrome bc_1 (*closed squares*) compared with the A101C-SL bound the wild type cytochrome bc_1 (*open circles*, replotted from *A*). Normalized fractions of bound cytochrome *c* in *A–C* were calculated from the decomposition of CW EPR similar to those shown in Fig. 2, as described under "Experimental Procedures," and in Fig. 5. For clarity, the *solid lines* show the trend fitted to the empirically derived equation described in supplemental Equation 4. The error of the estimations does not exceed 8%.

TABLE 2

Spin lattice relaxation time constants measured for cytochrome c_2 A101C-SL in the presence of cytochrome bc_1

ND, not determined.

NaCl	τ_1[a]	τ_2[b]	Lifetime[c]
mM	*μs*	*μs*	*μs*
0	3.27 ± 0.18	1.70 ± 0.25	~100
20	2.80 ± 0.10	1.20 ± 0.26	~10
40	2.35 ± 0.10	0.1 ± 0.05	~1
60	2.31 ± 0.03	ND	
80	2.37 ± 0.03	ND	
100	2.4 ± 0.05	ND	

[a] Time constant of the first exponent.
[b] Time constant of the second exponent.
[c] Estimated lifetime of the cytochrome c_2 associated with cytochrome bc_1.

than the SL relaxation rate, the SR curve becomes single exponential, and the averaged time constant and the bound and free components are no longer resolvable.

It thus appears that both SR EPR and CW EPR show a successive decrease of the bound cytochrome *c* as the ionic strength increases and neither method detects bound cytochrome *c* above 120 mM NaCl. This result can be interpreted in two ways. Either the long-lived complexes of cytochrome *c* with cytochrome bc_1 are not formed at detectable levels (the association rate constant decreases, whereas the dissociation rate constant is unaffected), or the complexes do form, but their lifetime is shorter than the snapshots of CW EPR measurements (the association rate constant decreases, whereas the dissociation rate constant increases).[3]

The EPR data provide two immediate indications that the hypothesis of short-lived complexes is the more likely. First, the relaxation time of A101C-SL in the presence of cytochrome bc_1 at high ionic strength (~2.37 ± 0.03 μs, Table 2) is longer than the relaxation time of A101C-SL in buffer without cytochrome bc_1 (~2.14 ± 0.04 μs, Table 1). This suggests that cytochrome *c* still interacts with cytochrome bc_1 at high ionic strength, and this interaction is sensed as the change in the relaxation rate even though the resolution of bound and free cytochrome *c* is difficult. Second, the limit above which the bound and free states cannot be separated by both methods is different (~40 mM NaCl for SR EPR and 120 mM NaCl for CW EPR). This shift seems to be the consequence of a successive decrease of the complex lifetime, first below the SR EPR snapshot and then below the CW EPR snapshot.

Indeed, this shift can be explained by the differences in the experimental time scales of SR EPR and CW EPR. SR EPR, governed by microseconds, would lose the separation of the dynamically exchanging bound and free states "earlier" (*i.e.* at lower ionic strength) than CW EPR, which extends the experimental resolution of those states down to the nanoseconds.

We thus can use the SR EPR and CW EPR data to approximate the limits of the complex lifetime at different ionic strengths. From one end, when the ionic strength is minimal,

[3] A third theoretical possibility, that the dissociation rate constant increases, whereas the association rate constant is unaffected, is not considered here, as it is unlikely that increase in ionic strength does not affect the association rate constant.

cytochrome *c* remains bound for more than 100 μs (Table 2).[4] From the other end, when the ionic strength corresponds to the physiological conditions, the complexes appear to last no longer than ~400 ns[5] with the association rate of cytochrome *c* approaching the time scale of its diffusion. The idea of the short-lived complexes finds further support when the SR and CW EPR data are analyzed in the context of cytochrome bc_1 enzymatic activity (see below).

Ionic Strength Dependence of Steady-state Kinetics of Cytochrome c Reduction by Cytochrome bc_1—As shown in Fig. 7, and well known from other studies (24, 57), the turnover rate of cytochrome bc_1 is greatly dependent on the ionic strength. This could be in part the result of the ionic strength influencing the binding of cytochrome *c* to cytochrome bc_1, a process known to involve the electrostatic interactions (24–26, 56).

When cytochrome c_2 was used as a substrate for cytochrome bc_1, the enzymatic activity showed a clear bell-shaped profile with a maximum turnover at around 150–200 mM NaCl and a progressive but quite moderate decrease from the maximum in both directions (Fig. 7). The rates with the yeast cytochrome *c* initially increased to reach a maximum turnover in a similar range of 150 to 200 mM NaCl. A further increase in ionic strength caused a decrease in the rates, which was much more pronounced than the decrease observed with cytochrome c_2. The rates with horse cytochrome *c* remained nearly constant in a range up to 100 mM NaCl and then, similar to yeast cytochrome *c*, showed a steep decrease. We noted that the activity of cytochrome bc_1 in reaction with physiological cytochrome c_2 did not drop more than 30% within the whole tested range (0–450 mM NaCl), whereas decreases of more than 80% were observed with nonphysiological mitochondrial cytochromes.

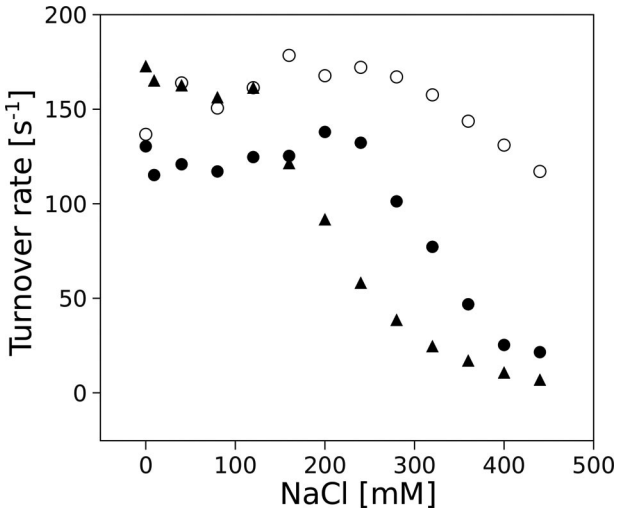

FIGURE 7. **Effect of ionic strength on cytochrome bc_1 enzymatic activity.** Steady-state turnover rates of reduction of *Rba. capsulatus* cytochrome c_2 (*open circles*), yeast cytochrome *c* (*closed circles*), and horse cytochrome *c* (*closed triangles*) by *Rba. capsulatus* cytochrome bc_1 are plotted as a function of salt (NaCl) concentration.

Regardless of those differences, all three profiles shown in Fig. 7 show that up to at least 100 mM NaCl cytochrome bc_1 remains highly active with close to maximum turnover rates. In the same range of ionic strength, the EPR measurements show a dramatic decrease of bound cytochrome *c* (Fig. 6, Table 2), which in principle could significantly compromise the enzymatic activity However, at salt concentrations where a minimal amount of or no bound cytochrome *c* is observed with EPR, enzymatic activity still remains at the maximum level. In other words, for a wide range of ionic strength conditions, the EPR measurements do not seem to resolve the interaction of cytochrome *c* with cytochrome bc_1, a prerequisite for electron transfer activity. This can be explained with the mode of interaction based on the short-lived complexes of cytochrome *c* with cytochrome bc_1. In this model, the complexes support the electron transfer even if the ionic strength shortens their lifetime down to the nanosecond time regime, where it is undetectable by EPR.

DISCUSSION

There are two aspects that need to be considered when describing the functional interaction of two redox proteins: the structural aspect of molecular association and the kinetic aspect of electron transfer. They are inherently coupled together and quite often not easy to be examined independently. It thus appears important that our dynamic picture of the molecular association of cytochrome *c* with cytochrome bc_1 was obtained from measurements that were fully independent of the electron transfer kinetics.

We propose that the transition from bound to free cytochrome *c* in the presence of cytochrome bc_1 detected by our EPR measurements (shown in Fig. 6 and Table 2) in fact reflects the natural process of the shortening of the lifetime of the complexes formed between these two proteins as the ionic strength increases. At low ionic strength the complexes last sufficiently

[4] The time constants of the experimental biexponential SR EPR recoveries represent an intrinsic relaxation rate modified by the presence of exchange according to the solutions of the Bloch (62) and McConnell equations (63). From CW EPR experiments one can estimate the value of the second order dissociation constant to be of the order of 10^{-6} M. At 0 mM NaCl the shorter time constant of the biexponential SR EPR recovery equals 1.7 μs (Table 2). It follows from the Bloch-McConnel equations that this corresponds to the first order association rate constant, $\sim 2 \times 10^5$ s^{-1}. For 63 μM cytochrome bc_1 mixed with 34 μM cytochrome c_2 in the absence of salt, the concentration of free cytochrome bc_1 is $\sim 3 \times 10^{-5}$ M. Thus the second order association rate constant can be estimated to be in the range of 6×10^9 s^{-1} M^{-1}. It follows that at the low ionic strength, when the fraction of bound cytochrome c_2 approaches unity, the dissociation rate constant has to be much slower than the association rate constant and does not exceed 1×10^4 s^{-1}. Thus cytochrome c_2 remains bound for more than 100 μs. Those values for the association and dissociation rate constants are in good agreement with published data (27).

[5] CW EPR spectra recorded at different ionic strengths can be reproduced by a linear combination of spectra for the predominantly bound and unbound states of cytochrome c_2 (Fig. 5). Thus, it can be deduced that exchange rates between those states are much slower than the transverse relaxation rates that determine the shape of the CW spectra. It follows from Fig. 6 that above 120 mM NaCl, less then 5% of bound cytochrome c_2 can be detected. Thus the second order dissociation constant for the cytochrome c_2-cytochrome bc_1 complex exceeds 1 mM. For 40 μM cytochrome bc_1 the first order dissociation constant is greater than 25. It follows that the first order dissociation rate constant should be at least 25 times faster than the corresponding first order association rate constant. At that concentration of cytochrome bc_1 and with the diffusion constant of cytochrome c_2 of 2×10^{-6} cm^2/s, the first order association rate constant can be estimated to be on the order of 10^5 s^{-1}, which agrees with the published data (64). Thus the dissociation rate should be in the range of 2.5×10^6 s^{-1} and the average lifetime of the cytochrome c_2-cytochrome bc_1 complex on the order of 400 ns.

long (more than 100 μs) to become detectable by EPR, whereas at high ionic strength (above ~120 mM NaCl) their lifetime falls below 400 ns. As a consequence the dissociation constant increases and the steady state fraction of bound cytochrome c_2 falls below the detection limit of CW EPR spectroscopy.

This picture is consistent with the light-induced kinetic measurements, which show that rapid intracomplex electron transfer, reminiscent of cytochrome *c* bound to cytochrome bc_1 prior to the activation, is prominent only at low ionic strength (23, 27). As the ionic strength increases, the intracomplex phase disappears concomitantly with an appearance of a bimolecular reaction between a bulk cytochrome *c* and cytochrome bc_1. The kinetically defined transition from the intracomplex to bimolecular electron transfer occurs within a range of ionic strength similar to the transition defined by our EPR measurements, *i.e.* above ~80 mM NaCl no intracomplex electron transfer was observed (23, 27).

The submicrosecond time scale of the dissociation rate of cytochrome *c* from cytochrome bc_1 may appear very fast; however, one needs to consider that with EPR spectroscopy we could observe only a part of the whole process of molecular association. This is because the SL attached to cytochrome *c* detects changes only if its rotation is damped by a *tight* binding, which is usually considered to be the final step of the association (14, 16). The steps that precede this final step, including a formation of the encounter complex and its evolution into the final, tightly bound complex, may have escaped our EPR measurements. This is because an estimated separation of the interacting molecules within the encounter complex can be as large as 1 nm (14, 16), which is more than enough to remove the mobility restrictions of the SL attached to cytochrome *c* used by our EPR measurements to report a binding. Obviously, the same holds true for conditions in which all of the attractions of two proteins are lost, which is believed to occur when two molecules are more than ~2 nm apart (16).

Thus, our estimates on the lifetime of the complex should be regarded as relating to the tightly bound complex and its transition to the encounter complex. It appears that at physiological ionic strength (around 100 mM) the tight complexes last no longer than hundreds of nanoseconds, and thus the association rate of cytochrome *c* approaches the time scale of its diffusion. This has important consequences on the mechanisms of interaction of cytochrome *c* with cytochrome bc_1. In principle, it revitalizes an early idea of diffusion-coupled reactions that link the soluble electron carriers with the membranous complexes in electron transport chains (60, 61).

Fig. 8 summarizes the plausible predictions on how this coupling may be realized for conditions where the collisions between proteins are modulated by long-range electrostatic attractive forces. At low ionic strength, the surface-exposed charges of two interacting proteins secure the complementarity of the docking surfaces, which helps to direct the two molecules so that the cofactors are within a distance short enough to support physiologically competent electron transfer. However, the electrostatically attracted proteins remain tightly bound for a significant period of time, and a slow dissociation may limit the turnover rate even though the efficiency of a single electron transfer reaction per single collision event is high. A moderate

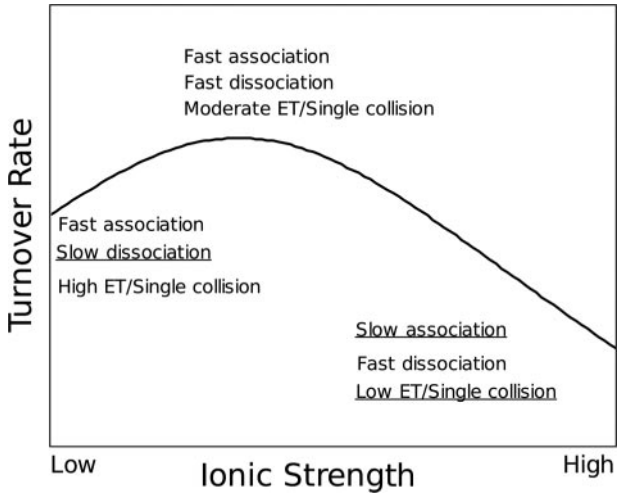

FIGURE 8. **Microscopic processes affecting the enzymatic turnover rate.** When collisions between redox proteins are modulated by long-range electrostatic attractive forces, the ionic strength influences processes of association and dissociation and efficiency of electron transfer (*ET*) per single collision. Processes limiting the turnover rate for conditions of low and high ionic strength are *underlined*.

increase in the ionic strength helps to increase the dissociation rate while maintaining some level of orientation guidance through the electrostatic attraction forces that remain sufficiently strong. This in part compromises the efficiency of electron transfer per single collision but, on the other hand, enhances cytochrome *c* exchange allowing the enzyme to reach the maximum turnover rates. A further increase in the ionic strength eliminates the electrostatic attractions altogether making the collision totally random and multidirectional. This significantly lowers the efficiency of electron transfer per single collision and decreases the turnover rates.

The diffusion-coupled mechanism of interaction has clear advantages for the multiple turnover of a redox enzyme working under physiological conditions. The bell-shaped profile of the enzymatic activity (Fig. 8) reaches a maximum at moderate ionic strength, which corresponds to the typical physiological conditions. At the same time, the robust interactions between the redox partners secure efficient turnover over a wide range of ionic strength conditions (which is often observed experimentally; see Fig. 7 (*open circles*) and examples in Refs. 24 and 57). These interactions should have a significant level of engineering tolerance, and the multiple turnover rates should not be that sensitive to the single mutations within the interacting surfaces. Indeed, the experimentally introduced point mutations tend to affect single turnover kinetics rather than enzymatic turnovers or functionality (24, 36).

Our estimates on the lifetimes of the tight complexes formed between cytochrome *c* and cytochrome bc_1 implicate important constrains on the electron transfer *per se*. At low ionic strength, the complexes last sufficiently long to satisfy the time requirement defined by an estimated electron transfer rate on the order of 10^6 s^{-1} (11). Intriguingly, this upper limit, predicted from a close spatial arrangement of hemes in the structure of cytochrome bc_1 co-crystallized with cytochrome *c* (11), has never been observed experimentally. It thus remains to be seen why the fastest rates recorded thus far, on the order of 10^4

s^{-1}, are 1–2 orders of magnitude slower (23, 27). On the other hand, at ionic strength above 120 mM NaCl, the average lifetime of the tight complex appears to be significantly shorter than the time needed for a single electron exchange between hemes *c* and c_1. This indicates that this exchange must be the product of several collisions of cytochrome *c* with cytochrome bc_1, consistent with the scheme shown in Fig. 8. At this stage the question of whether these collisions include just the oscillations within the radius of the encounter complex or also include an exchange with free cytochrome *c* in solution cannot be decided. Nevertheless, it is important to remember that electrons will tunnel in any direction to any redox center providing there is a net favorable driving force with a rate that has an approximately exponential dependence on distance (12, 13). We thus should expect that physiologically competent electron transfer takes place from more than just one conformation of the cytochrome *c*-cytochrome bc_1 complex.

A corollary of the diffusion-coupled mechanism is that cytochrome *c* (and any other soluble electron carrier) acts as a redox pool rather than a single molecule with a given redox state. Thus, we expect individual association and dissociation events to occur quite independently of the redox state of the interacting partners. This is consistent with the observation that the change in the redox state of heme c_1 does not significantly affect the lifetime of the complexes at physiological ionic strengths, as seen in the EPR measurements (Fig. 6*C*). Our EPR results show no indication of a conformational control over cytochrome *c* binding through the movement of the FeS head domain (22) nor of a long-range coordination of the binding through the Q_i catalytic site (11) for the conditions of physiological ionic strength. In fact, the nanosecond lifetime of the complexes would make such processes difficult. Instead, in our view, the diffusional communication of the substrate redox pools with membranous complexes provides sufficient and robust means to regulate electron flow through cytochrome bc_1 and, possibly, other components of the electron transport chains.

REFERENCES

1. Nicholls, D. G., and Ferguson, S. J. (2002) *Bioenergetics 3*, Academic Press, London
2. Moore, G. R., and Pettigrew, G. W. (1990) *Cytochromes C: Evolutionary, Structural and Physicochemical Aspects*, Springer-Verlag, Berlin
3. Rich, P. R. (2003) *Biochem. Soc. Trans.* **31,** 1095–1105
4. Haehnel, W. (1984) *Annu. Rev. Plant Physiol.* **35,** 659–693
5. Nelson, N., and Ben-Shem, A. (2004) *Nat. Rev. Mol. Cell Biol.* **5,** 1–12
6. Meyer, T. E., and Cusanovich, M. A. (2003) *Photosynth. Res.* **76,** 111–126
7. Kerfeld, C. A., and Krogmann, D. W. (1998) *Annu. Rev. Plant Physiol. Plant Mol. Biol.* **49,** 397–425
8. Ciurli, S., and Musiani, F. (2005) *Photosynth. Res.* **85,** 115–131
9. Daldal, F., Deshmukh, M., and Prince, R. C. (2003) *Photosynth. Res.* **76,** 127–134
10. Axelrod, H. L., and Okamura, M. L. (2005) *Photosynth. Res.* **85,** 101–114
11. Lange, C., and Hunte, C. (2002) *Proc. Natl. Acad. Sci. U. S. A.* **99,** 2800–2805
12. Moser, C. C., Keske, J. M., Warncke, K., Farid, R. M., and Dutton, P. L. (1992) *Nature* **355,** 796–802
13. Page, C. C., Moser, C. C., Chen, X., and Dutton, P. L. (1999) *Nature* **402,** 47–52
14. Harel, M., Cohen, M., and Schreiber, G. (2007) *J. Mol. Biol.* **371,** 180–196
15. Miyashita, O., Onuchic, J. N., and Okamura, M. Y. (2004) *Proc. Natl. Acad. Sci. U. S. A.* **101,** 16174–16179
16. Selzer, T., and Schreiber, G. (2001) *Proteins* **45,** 190–198
17. Meyer, T. E., Zhao, Z. G., and Cusanovich, M. A. (1993) *Biochemistry* **32,** 4552–4559
18. Zhou, H. (1993) *Biophys. J.* **64,** 1711–1726
19. Tetreault, M., Cusanovich, M. A., Meyer, T. E., Axelrod, H., and Okamura, M. Y. (2002) *Biochemistry* **41,** 5807–5815
20. Osyczka, A., Nagashima, K. V. P., Sogabe, S., Miki, K., Shimada, K., and Matsuura, K. (1999) *Biochemistry* **38,** 15779–15790
21. Osyczka, A., Nagashima, K. V. P., Sogabe, S., Miki, K., Shimada, K., and Matsuura, K. (2001) *J. Biol. Chem.* **276,** 24108–24112
22. Devanathan, S. S., Salamon, Z., Tollin, G., Fitch, J. C., Meyer, T. E., Berry, E. A., and Cusanovich, M. A. (2007) *Biochemistry* **46,** 7138–7145
23. Engstrom, G., Rajagukguk, R., Saunders, A. J., Patel, C. N., Rajagukguk, S., Merbitz-Zahradnik, T., Xiao, K., Pielak, G. J., Trumpower, B., Yu, C. A., Yu, L., Durham, B., and Millet, F. (2003) *Biochemistry* **42,** 2816–2824
24. Guner, S., Willie, A., Millett, F., Caffrey, M. S., Cusanovich, M. A., Robertson, D. E., and Knaff, D. B. (1993) *Biochemistry* **32,** 4793–4800
25. Hall, J., Kriaucionas, A., Knaff, D., and Millett, F. (1987) *J. Biol. Chem.* **262,** 14005–14009
26. Rieder, R., and Bosshard, H. R. (1980) *J. Biol. Chem.* **255,** 4732–4739
27. Tian, H., Sadoski, R., Zhang, L., Yu, C. A., Yu, L., Durham, B., and Millett, F. (2000) *J. Biol. Chem.* **275,** 9587–9595
28. Columbus, L., and Hubbell, W. L. (2002) *Trends Biochem. Sci.* **27,** 288–295
29. Fajer, P. G. (2000) in *Encyclopedia of Analytical Chemistry*, pp. 5725–5761, Willey & Sons Ltd., London
30. Feix, J. B., and Klug, C. S. (1998) in *Biological Magnetic Resonance*, Vol. 14, pp. 251–281, Plenum Press, New York
31. Atta-Asafo-Adjei, E., and Daldal, F. (1991) *Proc. Natl. Acad. Sci. U. S. A.* **88,** 492–496
32. Darrouzet, E., Mandaci, S., Li, J., Qin, H., Knaff, D. B., and Daldal, F. (1999) *Biochemistry* **38,** 7908–7917
33. Jenney, F. E., and Daldal, F. (1993) *EMBO J.* **12,** 1283–1292
34. Myllykallio, H., Jenney, F. E., Moomaw, C. R., Slaughter, C. A., and Daldal, F. (1997) *J. Bacteriol.* **179,** 2623–2631
35. Myllykallio, H., Zannoni, D., and Daldal, F. (1999) *Proc. Natl. Acad. Sci. U. S. A.* **96,** 4348–4353
36. Caffrey, M. S., Davidson, E., Cusanovich, M. A., and Daldal, F. (1992) *Arch. Biochem. Biophys.* **292,** 419–426
37. Bartsh, R. G. (1971) *Methods Enzymol.* **23,** 344–363
38. Valkova-Valchanova, M. B., Saribas, A. S., Gibney, B. R., Dutton, P. L., and Daldal, F. (1998) *Biochemistry* **37,** 16242–16251
39. Margoliash, E., and Frohwirt, N. (1959) *Biochem. J.* **71,** 570–572
40. Berliner, L. J., Grunwald, J., Hankovszky, H. O., and Hideg, K. (1982) *Anal. Biochem.* **119,** 450–455
41. Turyna, B., Osyczka, A., Kostrzewa, A., Blicharski, W., Enghild, J. J., and Froncisz, W. (1998) *Biochim. Biophys. Acta* **1386,** 50–58
42. Kooser, R. G., Kirchman, E., and Matkov, T. (1992) *Concepts Magn. Reson. A* **4,** 145–152
43. Sarewicz, M., Szytula, S., Dutka, M., Osyczka, A., and Froncisz, W. (2008) *Eur. Biophys. J.* **37,** 483–493
44. Ilnicki, J., Koziol, J., Oles, T., Kostrzewa, A., Galinski, W., Gurbiel, R. J., and Froncisz, W. (1995) *Mol. Phys. Rep.* **5,** 203–207
45. Froncisz, W., and Hyde, J. S. (1982) *J. Magn. Reson.* **47,** 515–521
46. Heckert, N. A., and Filliben, J. J. (2003) *NIST Handbook 148: DATAPLOT Reference Manual,* Vol. I, National Institute of Standards and Technology, Gaithersburg, MD
47. Hansen, D. F., and Led, J. J. (2003) *J. Magn. Reson.* **163,** 215–227
48. Berry, E. A., Huang, L.-S., Saechao, L. K., Pon, N. G., Valkova-Valchanova, M. B., and Daldal, F. (2004) *Photosynth. Res.* **81,** 251–275
49. Benning, M., Wesenberg, G., Caffrey, M. S., Bartsh, R. G., Meyer, T. E., Cusanovich, M. A., Rayment, I., and Holden, H. M. (1991) *J. Mol. Biol.* **220,** 673–685
50. DeLano, W. L. (2002) The PyMOL Molecular Graphics System, DeLano Scientific, San Carlos, CA
51. Biswas, R., Kühne, H., Brudvig, G. W., and Gopalan, V. (2001) *Sci. Prog.* **84,** 45–67
52. Altenbach, C., Greenhalgh, D. A., Khorana, H. G., and Hubbel, W. L. (1994) *Proc. Natl. Acad. Sci. U. S. A.* **91,** 1667–1671

53. Altenbach, C., Froncisz, W., Hemker, R., McHaourab, H., and Hubbel, W. L. (2005) *Biophys. J.* **89,** 2103–2112
54. Kostrzewa, A., Pali, T., Froncisz, W., and Marsh, D. (2000) *Biochemistry* **39,** 6066 – 6074
55. Mailer, C., Nielsen, R., and Robinson, B. H. (2005) *J. Phys. Chem. A* **109,** 4049 – 4061
56. Hall, J., Zha, X., Yu, L., Yu, C. A., and Millett, F. (1987) *Biochemistry* **26,** 4501 – 4504
57. Hunte, C., Solmaz, S., and Lange, C. (2002) *Biochim. Biophys. Acta* **1555,** 21–28
58. Diaz-Moreno, I., Diaz-Quintana, A., De la Rosa, M. A., Crowley, P. B., and Ubbink, M. (2005) *Biochemistry* **44,** 3176 –3188
59. Maneg, O., Malatesta, F., Ludwig, B., and Drosou, V. (2004) *Biochim. Biophys. Acta* **1655,** 274 –281
60. Gupte, S., Wu, E. S., Hoechli, L., Hoechli, M., Jacobson, K., Sowers, A. E., and Hackebrock, C. R. (1984) *Proc. Natl. Acad. Sci. U. S. A.* **81,** 2606 –2610
61. Hackenbrock, C. R., Chazotte, B., and Gupte, S. S. (1986) *J. Bioenerg. Biomembr.* **18,** 331–368
62. Bloch, F. (1946) *Phys. Rev.* **70,** 460 – 474
63. McConnell, H. M. (1958) *J. Chem. Phys.* **28,** 430 – 431
64. Millett, F., and Durham, B. (2004) *Photosynth. Res.* **82,** 1–16